Frequency Dependence of Attenuation in Ground-Penetrating Radar: Insights from the Bishop Tuff.

Robert Grimm, Cynthia Dinwiddie, David Stillman, and Ronald McGinnis, Southwest Research Institute

Summary

Total attenuation in ground-penetrating radar (GPR) was directly measured in radargrams of the Bishop Tuff, CA, from 12.5–200 MHz. The weak variation of attenuation with frequency reaffirms the "GPR Plateau" concept and argues against a constant-Q model. Electrolytic absorption —determined using collocated DC resistivity profiling/ sounding—accounts for about half of the attenuation and is by definition independent of frequency. The radargrams contain numerous reflections interpreted to be subvertical and subhorizontal cooling and unloading joints, suggesting that scattering is the other major contributor to attenuation. The residual attenuation after subtraction of absorption is attributed to scattering: significant variations in scattering attenuation are restricted to the decade around 30 MHz and are well fit by a Born scattering model.

Introduction

Attenuation in GPR is often considered to be proportional to frequency, i.e., the loss tangent or its reciprocal, the quality factor Q, is constant (Turner and Siggins, 1994; Noon et al., 1998; Irving and Knight, 2003). Yet constant Q has only limited applicability given the physical mechanisms of attenuation: it follows from laboratory measurements where multiple dielectric or magnetic relaxations are inferred to be superposed and it appears from theory in the diffusion regime. The latter can be discarded here as the realm of low-frequency electromagnetics. Electrolytic absorption from dissolved solids in groundwater generally dominates GPR absorption, and is independent of frequency *f*. The dielectric relaxation of water produces a frequency-squared absorption above several hundred megahertz going toward the maximum loss at ~17 GHz. These last two mechanisms, combined with the low-frequency falloff due to diffusion, are the foundation of the "GPR Plateau" that controls field measurement (Annan, 2005; Fig. 1, left). If losses followed constant Q, the GPR plateau would not exist. We define effective conductivity as the equivalent for any frequency-independent attenuation mechanism.

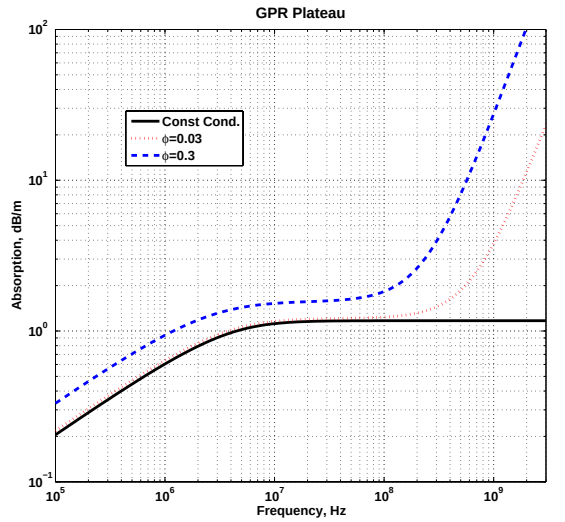

Figure 1. Theoretical framework for three regimes of absorption η with frequency *f*: diffusion (left, $\eta \propto f$), GPR plateau due to electrolytic loss (center, η = const) and dielectric relaxation of water (right, $\eta \propto f^2$). Porosity ϕ is saturated with water containing 0.01% dissolved solids. Background conductivity of 1.4 mS/m is used for comparison with Annan (2005).

Because electrolytic absorption is so important to GPR loss, it has been supposed that the lack of water near the surfaces of other planets will result in very deep radar-wave penetration. Sounding radars are currently operating from orbit around Mars (Seu et al., 2002; Picardi et al., 2005): while the cold and relatively pure ice of the polar caps has been imaged, there has been no unambiguous published indication of such penetration in rock or regolith. Distinction between constant-Q and constant effective conductivity is even more important for orbital ground-penetrating radars, because geometric spreading is negligible in the subsurface and so depth of investigation follows directly from attenuation. Constant-Q attenuation in this case predicts depth falling off faster than 1/*f* (attenuation proportional to frequency, plus frequency-squared term in radar-range equation), which contributed to the selection of very low operating frequencies (<25 MHz). Where attenuation is nearly independent of frequency, whatever the mechanism, depth of investigation only decreases slowly with frequency (e.g., as ~1/4 power for an planar reflector). Thus the implication is to select as high an operating frequency as possible for maximum resolution and expect adequate penetration depths.

In 2004 we undertook a campaign of GPR and supporting geophysical surveys in Mars-analog environments in order to better understand the fundamental controls on GPR attenuation and depth of investigation. The Volcanic Tableland of the Bishop Tuff (Fig. 2) was among the sites studied based on its arid environment, likely deep water table, Mars-analog rocks, and extensive prior geological characterization (see Grimm et al., 2006; Dinwiddie et al.,

Figure 2. Volcanic Tableland of the Bishop Tuff and surroundings. Astronaut photo from STS–073, Frame 5117, NASA. "Field Site" indicates location of Site 2, one of six individual sites studied here.

2006; 2007). Transient electromagnetic (TEM) soundings confirmed a deep water table, but subsequent Schlumberger DC resistivity soundings indicated that shallow resistivities averaged ~500-2000 Ω-m. Conductivity is therefore high enough that electrolytic absorption due to vadose-zone moisture still plays a role in GPR attenuation at this site. Our objective is to identify and quantify the principal attenuation mechanisms and explore their implications for both terrestrial and planetary GPR.

GPR Surveys

We performed GPR surveys at the Volcanic Tableland in two phases. In November 2004, data were acquired at three sites using a Sensors and Software PulseEkko 100 at frequencies of 12.5, 25, and 50 MHz, and a GSSI Multiple Low Frequency (MLF) system at 20, 40, and 80 MHz. In July 2006 we returned to Site 2 of the previous survey (Fig. 2) and resurveyed the line with the PulseEkko at 50, 100, and 200 MHz as well as with a GSSI radar at 270, 500, and 900 MHz. A detailed dipole-dipole resistivity survey was also performed on Line 2 using a 96-channel Syscal Pro resistivity meter.

The GPR record sections show numerous reflectors (e.g., Fig. 3). At lower frequencies (<100 MHz), hyperbolae and inverted V's dominate, both are indicative of laterally compact scatterers. At higher frequencies, more structure is evident, including discontinuous subhorizontal reflectors. We interpret the inverted V's as subhorizontal waves reflecting from near-surface subvertical contacts, likely cooling joints. Subhorizontal reflectors are also probably either cooling or unloading joints with a few contacts from known variations in tuff lithology.

The ubiquity of reflectors in these surveys suggests that scattering is an important attenuation mechanism. Scattering is likely dominant within dry planetary bodies where dielectric or magnetic relaxations are absent. After measuring the total attenuation in the record sections, we subtract absorption and model the residual as scattering.

Attenuation Analysis

Where reflectors are separated by a few wavelengths or less, scattering is nearly continuous and average amplitudes appear to decrease continuously. A continuous terminal wavetrain has long been recognized in earthquake seismology as a scattering coda (e.g., Aki and Chouet, 1975). We previously reported the attenuation measured in the "coda Q" from 12.5–50 MHz (Grimm et al., 2006); here we add results from 50–200 MHz and demonstrate that the residual attenuation following subtraction of absorption is indeed well fit by a simple scattering model.

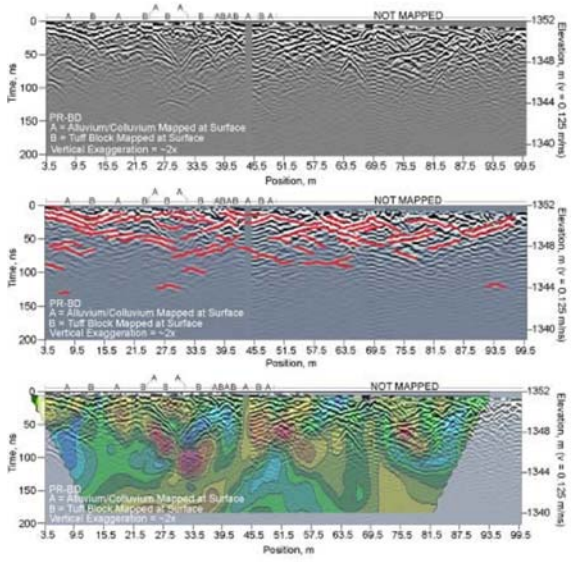

Figure 3. Bishop Tuff Line 2, 200 MHz. Top: Unmigrated radargram. Middle: Mapped reflectors, interpreted as cooling and unloading joints. Bottom: With superposed resistivity (range 100-5000 Ω-m). "A/B/Not Mapped" codes at top refer to surficial geology (see Dinwiddie et al., 2007).

In order to measure the coda Q, we compress the radargram to a single time-dependent function by taking the mean square over all traces in the record section: this is the energy average trace. This operation implicitly assumes that the medium is composed of horizontal layers and/or isotropic random scatters. Time-depth conversions were made using CMP soundings. The energy-average trace is corrected for geometric spreading and for the backscatter cross-section. The resulting curves show a clean segment of continuous semilogarithmic amplitude decay with time (e.g., Fig. 4). The slope of this curve is the total attenuation in dB/m: both scattering and absorption determine the total loss. The total attenuation from 12.5–200 MHz, and the depth intervals to which they apply, are given in Table 1. The GSSI data were not suitable for this analysis due to strong reverberation and uncertainty in the intrinsic gain functions.

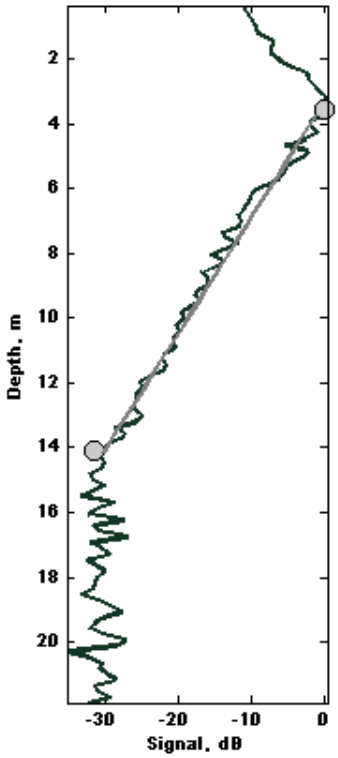

Figure 4. Average energy with depth for Volcanic Tableland Site 2, PulseEkko, 50 MHz, following backscatter cross-section and geometric spreading corrections. Fit linear segment is the scattering coda, whose slope is the total attenuation (dB/m, scattering + absorption).

Absorption

The attenuation due to absorption (Table 1) was calculated from the dipole-dipole resistivity survey (Fig. 3), first by computing the average resistivity ρ over the depth interval for which the coda-Q measurement was made and then converting to dB/m = $1640/\rho\sqrt{\varepsilon_r}$, where the dielectric constant $\varepsilon_r \approx 7$ at this site from CMP radar soundings. This formula applies to absorption loss tangents $<<1$ and is satisfied here for all cases. Average resistivities of 800–1000 Ω-m over the radar investigation depths translate to 0.6–0.7 dB/m of absorption. The residual attenuation following subtraction of absorption is taken to be the scattering attenuation.

Scattering

For a typical inferred scattering attenuation $\eta = 0.8$ dB/m for this site, the mean-free path between scatterers $L = 4.34/\eta = 5$ m (see Grimm et al., 2006, and references therein). This is in reasonable agreement with the scale of jointing mapped in the radargrams and at the surface (Fig. 2; see Dinwiddie et al., 2007).

We further pursue quantitative analysis of scattering using a simple Born model (see Aki and Chouet, 1975, and references therein), which assumes single scattering in a weakly heterogeneous medium. Velocity heterogeneity ξ is specified using either an exponenential $\exp(-r/a)$ or gaussian $\exp(-r^2/a^2)$ autocorrelation function, where r is distance and a is the correlation length. Both autocorrelation functions produce Rayleigh scattering (scattered power increasing as f^4) at low frequency, but differ at high frequency: the extended exponential shape function leads to a geometric optics limit (constant scattering attenuation) at high frequency, whereas the compact gaussian shape function backscatters energy less efficiently and exhibits decreasing attenuation at high frequency. The optimal Born scattering parameters ξ and a were determined by a simple grid search. The effective frequency (Table 1) was the location of the energy peak in a spectral analysis; it is lower than the center frequency due to imperfect ground coupling.

We find that the Born scattering model using the exponential autocorrelation function produces a good fit to the Volcanic Tableland Site 2 GPR data, with $\xi = 0.34$ and $a = 1$ m. Physically, these parameters again support the inference that substantial scattering heterogeneity occurs on length scales of meters.

An important corollary is that the asymptotic frequency limit to which the scattering attenuations appear to be trending is predicted by the geometric optics limit for the

exponential autocorrelation. The gaussian autocorrelation predicts a downturn in attenuation akin to a relaxation that is not observed at 200 MHz and below. In spite of being unable to use the GSSI radargrams for coda-Q analysis, we attempted to use these data simply to test the hypothesis that attenuation was constant at 270–900 MHz using radar-range analysis. Although still troubled by data quality, the biggest impediment to this test was that the depth of investigation at high frequency (a few meters) was less than the typical separation of reflectors in the radargrams, so that reflectors defining the maximum depth of investigation could not always be found. We continue to pursue radar-range analysis as a simple alternative to coda-Q.

Conclusions

The Bishop Tuff proved to be a useful analog for studying both absorption and scattering in GPR. The total attenuation depended only weakly on frequency, confirming the "GPR Plateau" concept. About half of this loss is due to frequency-independent absorption. The frequency dependence of the residual attenuation is well modeled by Born scattering. The frequency dependence of scattering is also insignificant except in the decade centered on ~30 MHz. Scattering and absorption at this site—which together approximate a constant effective conductivity—dominate over any intrinsic relaxation mechanisms that might be considered constant-Q. The weak frequency dependence of attenuation implies that planetary sounding radars may only slowly give up depth of investigation with increasing frequency, with the benefit of much improved resolution.

Acknowledgements

This work was supported by Southwest Research Institute's Internal Research program and by NASA grants NNG05GM32G (CLD) and NNG05GL88G (REG). We thank our numerous colleagues who participated in the fieldwork and helpful discussions, and Essam Heggy in particular for acquiring the GSSI data.

Table 1. Attenuation Parameters for GPR Surveys at Bishop Tuff Volcanic Tableland Site 2

Nominal Freq., MHz	Effective Freq., MHz	Depth Inverval, m	Total Attenuation, dB/m	Resistivity, Ω-m	Absorption, dB/m	Scattering (Residual) Atten., dB/m	Scattering Albedo
12.5	12	11-22	0.95	990	0.62	0.33	34%
25	22	5-22	1.17	950	0.65	0.52	44%
50 (1)	36	5-14	1.40	930	0.67	0.73	52%
50 (2)	37	4-10	1.54	890	0.69	0.85	55%
100	90	3-9	1.75	890	0.70	1.05	60%
200	180	2-7	1.83	860	0.72	1.11	61%

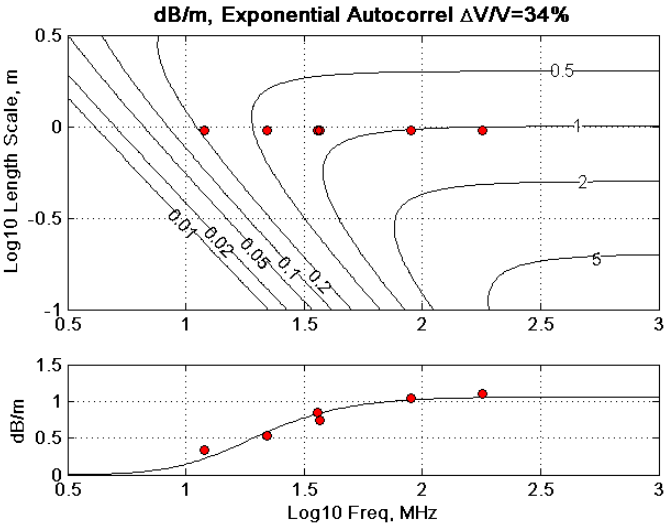

Figure 5. Born scattering model applied to GPR residual attenuation. Top: Contours of scattering loss in dB/m as functions of frequency and length scale, for best-fit characteristic velocity contrast of 34%. Red dots are GPR center frequencies shown at best-fit characteristic scale of velocity heterogeneity ~1 m. Bottom: Cross-section through top figure, showing dB/m loss as function of frequency with model fit. Note prediction of asymptotic loss in high-frequency geometric-optics limit.

References (Delete From Submitted Abstract)

Turner, G., and A.F. Siggins, 1994, Constant Q attenuation of subsurface radar pulses: Geophysics, **59**, 1192-1200.

Irving, J.D., and R.J. Knight, 2003, Removal of wavelet dispersion from ground-penetrating radar data: Geophysics, **68**, 960-970.

Bano, M., 2004, Modelling GPR waves for lossy media obeying a complex power law of frequency for dielectric permittivity: Geophysical Prospecting, **52**, 11-26.

Noon, D.A., G.F. Stickley, and D. Longstaff, 1998, A frequency-independent characterisation of GPR penetration and resolution performance: J. Appl. Geophysics, **40,** 127-137.

Annan, P., 2005, Ground-Penetrating Radar: in D.K. Butler, ed., Near Surface Geophysics, Society of Exploration Geophysics Investigations in Geophysics No. 13, 357-438.

Dinwiddie, C.L., 2006, EOS Trans. AGU.,

Dinwiddie, C.L., R.E. Grimm, R.N. McGinnis, and D.E. Stillman, 2007, Moderately to poorly welded tuff, Bishop, California: Geophysical and geological characterization to determine the source of radar scattering: 7th Intl. Mars. Symp., California Inst. Technol.

Grimm, R.E., E. Heggy, S. Clifford, C. Dinwiddie, R. McGinnis, and D. Farrell, 2006, Absorption and scattering in ground-penetrating radar: Analysis of the Bishop Tuff: J. Geophys. Res., **111,** doi:10.1029/2005JE002619.

Picardi, G., and 33 others, 2005, Radar soundings of the subsurface of Mars: Science, **310**, 1925-1928.

Seu, R, D. Biccari, L.V. Lorenzoni, R.J. Phillips, L. Marinangeli, G. Picardi, A. Masdea, and E. Zampolini, 2004, SHARAD: The MRO 2005 shallow radar: Planetary and Space Science, **52**, 157-166.

Aki, K., and B. Chouet, 1975, Origin of coda waves: Source, attenuation, and scattering effects: J. Geophys. Res., **80**, 3322-3342.